PHYSICAL REVIEW B VOLUME 55, NUMBER 11 15 MARCH 1997-I

Quantum transport in δ-doped quantum wells

Guo-Qiang Hai and Nelson Studart
Departamento de Física, Universidade Federal de São Carlos, 13565-905, São Carlos, São Paulo, Brazil

(Received 11 September 1996)

The multisubband electron-transport properties are studied for GaAs/Al$_x$Ga$_{1-x}$As quantum wells in which a thin doping layer is located in the center. The subband transport mobility and quantum mobility are obtained as a function of the width of the quantum well and doping concentration. The effects of the screening and the intersubband interaction are investigated through the control of the number of the occupied subbands by adjusting the width of the quantum well and are shown to be relevant in the multisubband transport of the present system. The subband quantum mobility is enhanced significantly due to the occupation of the next higher subband. We found that the dependence of the transport and the quantum mobility of each subband on the well width and doping concentration exhibits nonmonotonic behavior with the appearance of a local maximum. [S0163-1829(97)02207-8]

In recent years there has been increasing interest in the study of the electron transport properties of the quasi-two-dimensional electron gas (Q2DEG) in δ-doped semiconductors.[1–7] The δ-doped systems are in general characterized by a rather high electron density, which makes them different from the other 2D systems. Typically, several subbands are occupied in a δ-doped system and effects resulting from the occupation of several subbands can be studied. In previous works, we studied the electron transport properties in single[7] and double[8] δ layers. The screening of the electron gas on the ionized impurity scattering potential was studied within the random-phase approximation (RPA). We found that, the intersubband coupling of the electron gas is essential in the screening effect to understand the multisubband transport properties.[7,9] Our calculation also showed that, by increasing the width of the doping layer, the mobility of the lowest subband increases as illustrated by Masselink[10] for the case of a doped quantum well (QW). However, the mobility of higher subbands exhibits a quite different behavior. New information on the electron transport properties associated with the δ-layer system can be obtained when it is subjected to additional confinement as in a QW. Due to such an extra confinement, the intersubband interaction is greatly enhanced.

In this paper, we report a study on the electron subband mobility in δ-doped QW systems. The effects of the width of the QW and the doping concentration on the subband transport and quantum mobilities are investigated. We will show many-body effects in the Q2DEG electron gas, which screens the ionized-impurity potential in this multisubband system. The advantage of studying the δ-doped QW system is that, by varying the width of the QW, one can easily control the number of populated subbands that make a direct contribution to the intersubband interaction. On the other hand, since the overlap between the wave functions of the electrons and the ionized impurities is related to the strength of the impurity scattering, we also can study the influence of the overlap on the electron subband mobilities. The present work addresses the effects of the intersubband interaction on the mobilities of the electrons in different subbands and the influence of the extra confinement due to the QW.

We consider a GaAs/Al$_x$Ga$_{1-x}$As QW structure with a thin doping layer located in its center. The offset of the conduction band is taken as $V_b = 0.6\times(1.155x + 0.37x^2)$ eV.[11] The impurities are distributed uniformly in the doping layer with areal concentration N_D and thickness $W_D = 10$ Å.

The electronic structure of the system is determined by employing the self-consistent calculation within the local density approximation.[7] Figure 1 shows the subband energy E_n as a function of width of the QW W_{QW} in the Si δ-doped GaAs/Al$_{0.3}$Ga$_{0.7}$As structure with $N_D = 5\times10^{12}$ cm^{-2} and the background acceptor concentration was taken as 10^{14} cm^{-3}. It is seen that the width of the QW alters the number of populated subbands. For small W_{QW}, only the lowest subband is populated. With increasing W_{QW} the distance between the two levels decreases and more subbands are populated. The subbands $n=2$ and 3 begin to be occupied at $W_{\mathrm{QW}} = 76$ and 215 Å, respectively. It is also interesting to notice that the Fermi energy of the highest occupied subband increases with increasing the width of the quantum well, but those of the lower subbands decrease.

The electron transport mobility and the quantum mobility are studied within the linear response theory.[7,12–15] In the calculation, only the scattering of the ionized donors in the doping layer is considered because it is the most important

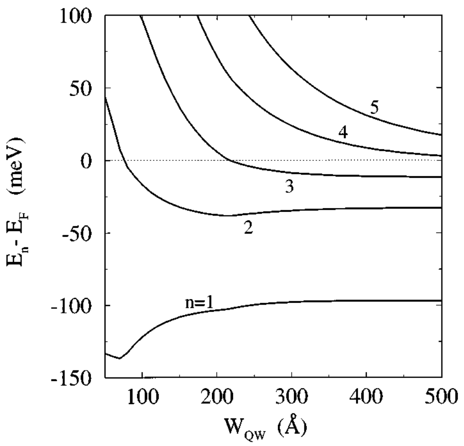

FIG. 1. The subband energy as a function of width of the QW for a Si δ-doped GaAs/Al$_{0.3}$Ga$_{0.7}$As QW structure with a doping layer of $N_D = 5\times10^{12}$/cm^2 and $W_D = 10$ Å located in the center.

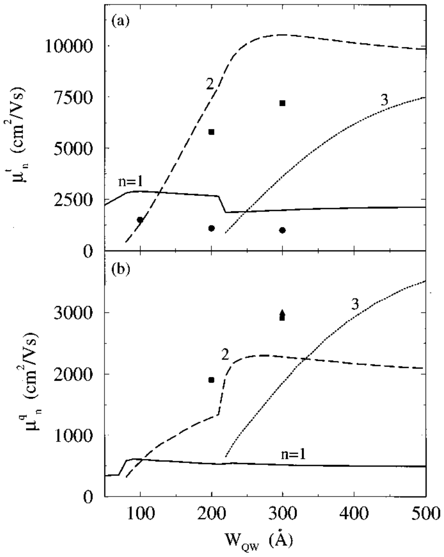

FIG. 2. The subband (a) transport mobility and (b) quantum mobility as a function of the width of the Si δ-doped GaAs/Al$_{0.3}$Ga$_{0.7}$As QW for $N_D = 5\times10^{12}/\text{cm}^2$. The experimental results (Ref. 5) are indicated by the solid circles, squares, and triangles corresponding to $n=1$, 2, and 3, respectively.

scattering mechanism at low temperature. The screening of the 2D electron gas on the impurity scattering is taken into account through the dielectric function within the RPA. As discussed in Ref. 7 for the δ-doped system, the empty subbands influence the electron mobility through the screening effects. In the present calculation, we included all the occupied subbands and two empty subbands above the Fermi energy E_F in the dielectric response function.

The subband transport mobilities μ^t_n, which are obtained by solving the Boltzmann equation, are depicted as a function of W_{QW} in Fig. 2(a). It is seen that, with increasing W_{QW}, the transport mobility of the lowest subband μ^t_1 increases until $W_{\text{QW}} = 100$ Å (the onset of occupation of the second subband occurs at $W_{QW} = 76$ Å) and then it decreases slowly. At the onset of occupation of the third subband, μ^t_1 has an abrupt decrease due to the onset of the intersubband scattering channel between the two subbands. The mobilities of the second and third subbands have a similar behavior as a function of W_{QW}. They are strongly influenced by the confinement of the QW. μ^t_2 increases fast with increasing W_{QW} until it reaches a maximum around $W_{\text{QW}} = 300$ Å and then decreases (the onset of occupation of the third subband is at $W_{\text{QW}} = 215$ Å). We also observe in Fig. 2 that μ^t_3 increases with the increase of W_{QW} for the well widths considered. The experimental results of the subband transport mobility of a Si δ-doped GaAs/Al$_{0.33}$Ga$_{0.67}$As QW, obtained by Harris, Murray, and Foxon,[5] are indicated by the solid circles and squares for the first $(n=1)$ and the second $(n=2)$ subbands, respectively. The thickness of the doped-impurity layer in the sample was less than 15 Å, and the measurement was done at 4.2 K. The subband transport mobilities were obtained from the so-called multiband Hall effect by fitting the results within the one- or two-subband models. For $W_{\text{QW}} = 300$ Å, three subbands are populated. The experimental data were inferred from the two-subband model by assuming that the second and the third subbands have the same transport mobility. By comparing our results with the experimental ones, it is seen that the calculated mobility is in qualitative agreement with the measurement results. Quantitatively, however, the calculated mobility for the lowest subband is about two times larger than the experimental results. On the other hand, the calculation shows that the second and the third subbands have quite different transport mobilities at $W_{\text{QW}} = 300$ Å. The data deduced from the measurements are almost in the middle of the calculated mobilities of the two subbands.

We note in Fig. 2(b) that the subband quantum mobilities μ^q_n, which are determined from the quantum lifetime or the single particle relaxation time, have distinct behavior as compared with the corresponding transport ones through the following observations: (i) the quantum mobility is smaller by a factor of 4–5 for the $n=1$ and 2 subbands, and about a factor of 2 for the $n=3$ subband; (ii) at the onset of the occupation of a higher subband, quantum mobility of the lower subband shows a pronounced fast increase; and (iii) $\mu^q_3 > \mu^q_2$ when $W_{\text{QW}} > 330$ Å but, for the transport mobility, $\mu^t_3 < \mu^t_2$ as long as the $n=4$ subband is unoccupied. μ^q_2 and μ^q_3 exhibit similar behavior, and μ^q_2 has a maximum at $W_{\text{QW}} = 270$ Å. At the onset of the occupation of a higher subband, the quantum mobility of the lower subband shows a rapid increase, which can be attributed to the screening effect related to the intersubband coupling. Such an effect is pronounced for scatterings with long wavelengths, i.e., the small-angle scattering. However, for the transport mobility, the scattering at small angles almost does not contribute to the process, but it is mainly determined by scattering at larger angles. By comparing the calculated quantum mobility with the results from the Shubnikov–de Haas measurements,[5] we see that our calculation shows similar results as compared to the experimental ones. The experiments indicate that μ^q_3 is slightly larger than μ^q_2 at $W_{\text{QW}} = 300$ Å. Our calculation shows that μ^q_2 and μ^q_3 may be very different depending on the width of the QW, but they are close to each other around $W_{\text{QW}} = 330$ Å. Quantitatively, the quantum mobility from our calculation is smaller than the experimental result.

An overall description of the results, shown in Fig. 2, of our calculations indicates that, by increasing the well width, both the transport and the quantum mobilities of the highest occupied subband are enhanced. We also observe that the transport mobility increases faster than the quantum mobility. This is a consequence of the fact that the increase of the well width leads to an increase of the Fermi energy of the highest occupied subband as shown in Fig. 1, or in other words, the kinetic energy of the conduction electrons on the Fermi surface becomes larger. This results in a decrease of the scattering rate, especially, for large-angle scatterings. In addition, by increasing W_{QW}, the overlap between the wave functions of the electron and the impurities decreases, leading to a reduction of the impurity scattering. On the contrary, the Fermi energy of the lower subbands decreases with increasing the well width. Moreover, the intersubband scattering is enhanced and the mobilities of the lower subbands decrease with increasing the well width.

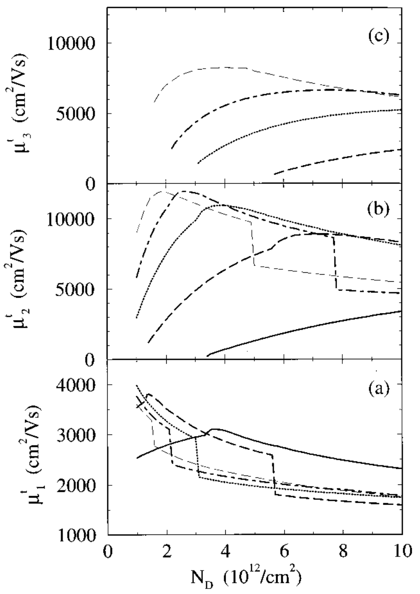

FIG. 3. The transport mobilities of the electrons in (a) the lowest subbands $(n=1)$, (b) the second subband $(n=2)$, and (c) the third subband $(n=3)$ as a function of the impurity concentration in the Si δ-doped GaAs/Al$_{0.3}$Ga$_{0.7}$As QW's of different widths. The solid, dashed, dotted, dash-dotted, and the thin-dashed curves indicate the results for the QW's of widths $W_{\text{QW}}=100$, 200, 300, 400 Å, and ∞, respectively.

The quantitative discrepancies between the theoretical and the experimental results could be attributed to several factors. It is well known that, in heavily doped semiconductors such as present system, the strong overlap among the impurities leads to a reduction of the band gap. Furthermore, the random distribution of the impurities results in disorder in the system. Gold, Ghazali, and Serre[16] showed that a band tail induced by the disorder appears in the density of states in δ-doped GaAs. We found that in Si δ-doped GaAs, the correlation between the screened Coulomb scattering potential should be pronounced for the doping concentration larger than $(2-3)\times10^{12}$ cm^{-2}.[17] However, impurity correlations and disorder effects on the electron transport properties in heavily doped systems are still not well understood. Other possible mechanisms, such as localized levels of DX centers and the nonmetastable levels[3,5] above the conduction-band edge, could influence the electronic structure and lead to a Fermi-level pinning in δ-doped semiconductors. Other scattering mechanisms at low temperature are the interface roughness of the heterojunctions, ionized acceptors, neutral impurities, and localized states induced by heavy doping. They can modify the electron transport properties. In our previous work, however, we showed that our calculations of the quantum mobility in single and double δ layers are in quite good agreement with the experimental results.[4,7–9] The experimental results of quantum mobilities in δ-doped QW's, taken from Ref. 5 and compared with our results, were obtained from the half-width of the Fourier peaks of the Shubnikov–de Haas oscillations. However in Refs. 4 and 9, the quantum mobility was measured by using a Fourier filtering technique together with the so-called Dingle plot. Generally, the latter method yields smaller relative error in the measured quantum mobilities.

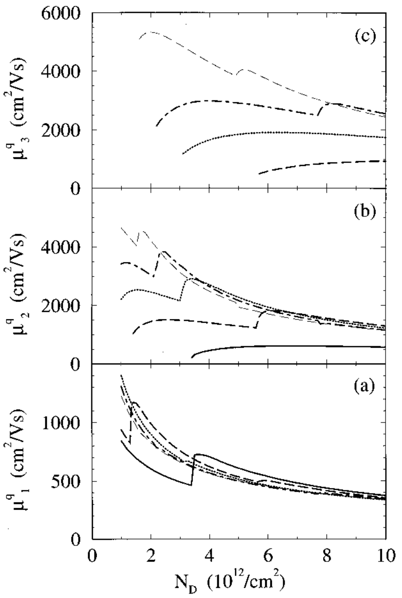

FIG. 4. The same as Fig. 3 but now for the subband quantum mobility.

Figure 3 shows the dependence of the subband transport mobility on the impurity concentration in δ-doped QW's with width $W_{\text{QW}}=$ 100, 200, 300, and 400 Å. For comparison, the transport mobility in a single δ layer, i.e., $W_{\text{QW}}=\infty$, is depicted by thin curves. We observe that μ_1^t increases with increasing the doping concentration when only the lowest subband is populated as can be seen for the QW's with widths of 100 and 200 Å. After the onset of the population of the second subband at $N_D=3.4\times10^{12}$ cm^{-2} for the 100-Å QW and $N_D=1.3\times10^{12}$ cm^{-2} for the 200-Å QW, μ_1^t increases up to a maximum and then it becomes a decreasing function. The increase of μ_1^t just after the onset of the occupation of the second subband is obviously due to the screening effect coming from the coupling of the two subbands. Notice that, because the wave functions of the two subband have different parities, the intersubband scattering between them is very small (it vanishes when the thickness of the doping layer is zero). Similarly, at the onset of the population of the third subband, which occurs at $N_D=$ 5.7, 3.1, 2.2, and 1.5×10^{12} cm^{-2} for the QW's with $W_{\text{QW}}=200$, 300, 400 Å, and infinity, respectively, the mobility μ_2^t increases quickly until it reaches a maximum at $N_D=$ 7.0, 3.8, 2.6, and 1.85×10^{12} cm^{-2}, and then it decreases with increasing N_D. We found that, with increasing N_D, μ_1^t decreases slowly as long as two or more subbands are populated. At the onset of the occupation of the $n=3$ subband, μ_1^t shows an abrupt decrease. This discontinuous decrease is a consequence of the intersubband scattering. We also see that such a jump becomes larger when the well width decreases. It indicates that the intersubband scattering strength is enhanced in narrower QW, in which the overlap of the wave function is larger. The abrupt decrease of μ_2^t at $N_D=7.8\times10^{12}$ cm^{-2} for $W_{\text{QW}}=400$ Å and $N_D=5.0\times10^{12}$ cm^{-2} for $W_{\text{QW}}=\infty$ is due to the onset of occupation of the $n=4$ subband. We also notice that this mobility drop is quite large. In Fig. 3(c), we see that μ_3^t has a similar behavior as μ_2^t shown in Fig. 3(b).

In Fig. 4, the subband quantum mobility is depicted as a function of the doping concentration for several QW's. The main differences of the quantum mobility μ_n^q from the transport mobility are (i) μ_1^q decreases with increasing N_D even if only the lowest subband is populated; (ii) a local maximum of μ_2^q appears before the onset of occupation of the $n=3$ subband; (iii) at the onset of the occupation of a higher subband, the quantum mobility of the lower subband shows a rapid increase. These different characteristics of the subband quantum mobility originate from the nature of the quantum mobility, which is dominated by the short-range scattering, while the screening of the Q2DEG is more efficient on the long-range scattering events. The abrupt increase of the subband quantum mobility at the onset of occupation of a higher subband reflects the screening effect on the scattering induced by a new populated subband, as discussed before, which is stronger than the intersubband scattering introduced by itself in the present system. The appearance of the local maximum in the subband quantum mobility as well as that in the transport mobility is also a consequence of the balance between the scattering and the screening effects.

In conclusion, we found that, except for the behavior of the subband mobilities around the onset of the occupation of a subband, there are two important factors that influence the electron transport when we increase the impurity concentration. One is that the electron density is increased and, consequently, the subband Fermi energy and the kinetic energy of the conduction electrons are increased, which leads to an enhancement of the mobility. The other is the scattering centers of the ionized donors increase, which leads to a decrease on the mobility. Since the increase of the Fermi energy mainly leads to a reduction of the large-angle scattering, with increasing the doping concentration, the transport mobility increases faster than the corresponding quantum mobility. Our results show that the screening effects of the Q2DEG and the intersubband scattering are of equal importance in the multisubband transport properties. We found that the transport and the quantum mobilities of each subband exhibit nonmonotonic behavior with a local maximum for the dependence on both the well width and doping concentration. We also want to mention that the barrier height of the QW does not influence significantly the subband mobility. The background acceptor concentration in the present system affects the subband mobility slightly as long as W_{QW} is not too large.

G.Q.H. was supported by the Conselho Nacional de Desenvolvimento Científico e Tecnológico (CNPq). The work was partially sponsored by the Fundação de Amparo à Pesquisa do Estado de São Paulo (FAPESP), Brazil.

---

[1] A. Zrenner, F. Koch, J. Leotin, M. Goiran, and K. Ploog, Semicond. Sci. Technol. **3**, 1132 (1988).

[2] E. F. Schubert, J. E. Cunningham, and W. T. Tsang, Solid State Commun. **63**, 591 (1987); E. F. Schubert, J. Vac. Sci. Technol. A **87**, 2980 (1990).

[3] E. Skuras, R. Kumar, R. L. Williams, R. A. Stradling, J. E. Dmochowski, E. A. Johnson, A. Mackinnon, J. J. Harris, R. B. Beall, C. Skierbeszewski, J. Singleton, P. J. van der Wel, and P. Wisnieski, Semicond. Sci. Technol. **6**, 535 (1991).

[4] P. M. Koenraad, A. C. L. Heessels, F. A. P. Blom, J. A. A. J. Perenboom, and J. H. Wolter, Physica B **184**, 221 (1993).

[5] J. J. Harris, R. Murray, and C. T. Foxon, Semicond. Sci. Technol. **8**, 31 (1993).

[6] X. Zheng, T. K. Carns, K. L. Wang, and B. Wu, Appl. Phys. Lett. **62**, 504 (1993).

[7] G.-Q. Hai, N. Studart and F. M. Peeters, Phys. Rev. B **52**, 8363 (1995); G.-Q. Hai and N. Studart, *ibid.* **52**, R2245 (1995).

[8] G.-Q. Hai, N. Studart, and F. M. Peeters, Phys. Rev. B **52**, 11 273 (1995).

[9] G.-Q. Hai, N. Studart, F. M. Peeters, P. M. Koenraad, and J. H. Wolter, J. Appl. Phys. **80**, 5809 (1996).

[10] W. T. Masselink, Phys. Rev. Lett. **66**, 1513 (1991).

[11] G.-Q. Hai, F. M. Peeters, and J. T. Devreese, Phys. Rev. B **42**, 11 063 (1990).

[12] S. Das Sarma and F. Stern, Phys. Rev. B **32**, 8442 (1985).

[13] S. Mori and T. Ando, Phys. Rev. B **19**, 6433 (1979); J. Phys. Soc. Jpn. **48**, 865 (1980).

[14] R. Fletcher, E. Zaremba, M. D'Iorio, C. T. Foxon, and J. J. Harris, Phys. Rev. B **41**, 10 649 (1990).

[15] H. L. Störmer, A. C. Gossard, and W. Wiegmann, Solid State Commun. **41** 707 (1982).

[16] A. Gold, A. Ghazali, and J. Serre, Semicond. Sci. Technol. **7**, 972 (1992).

[17] G.-Q. Hai and N. Studart (unpublished).